J. Mol. Model. **1999**, *5*, 169 – 176

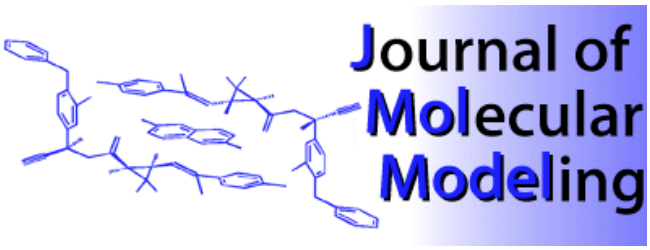

FULL PAPER

A Molecular Model of Inducible Costimulator Protein and Three-Dimensional Analysis of its Relation to the CD28 Family of T Cell-Specific Costimulatory Receptors

Jürgen Bajorath

New Chemical Entities, Inc., 18804 North Creek Pkwy. S., Bothell, WA, 98011-8805, and Department of Biological Structure, University of Washington, Seattle, WA 98195, USA. Tel: +1-425-424-7297; Fax: +1-425-424-7299; E-mail: jbajorath@nce-mail.com

Received: 20 July 1999/ Accepted: 20 August 1999/ Published: 14 September 1999

Abstract Inducible costimulator protein (ICOS) has recently been identified as a new member of the CD28 family of T cell costimulatory molecules. A molecular model of the extracellular immunoglobulin-like domain of ICOS was built based on the structure of CD152, another member of the CD28 family. Despite low sequence identity, ICOS shares consensus residues characteristic of immunoglobulin variable-type domains with CD152 and CD28 and also some unique features, suggesting that their three-dimensional structures are more similar to each other than to other proteins belonging to the immunoglobulin superfamily. The ICOS model was used to study sequence conservation in three dimensions and to compare the distribution of N-linked glycosylation sites in the extended CD28 family. The limited number of residues outside consensus/core positions that are conserved in ICOS and CD28 and/or CD152 are widely distributed over the extracellular domain. A few residues in CD152 and CD28 that are critical for binding of CD80/CD86 are also conserved in ICOS. However, the region in ICOS that corresponds to the CD80/CD86 binding site is masked by N-linked glycosylation. This suggests that this site is not available for binding of CD80/CD86 or other ligands. ICOS has probably diverged early from CD28 and CD152 and developed the capacity to recognize ligand(s) other than CD80/CD86, very likely utilizing a different molecular region and mechanism for binding.

Keywords Cell surface proteins, Comparative modelling, Functional regions, N-linked glycosylation, Immunoglobulin superfamily, Residue conservation, T cell costimulation

Introduction

CD28 [1] and CD152, also called CTLA-4 [2], are homologous type I transmembrane receptor proteins on T cells [3] and play a critical role in the regulation of T cell antigen receptor (TCR)-dependent immune responses [3,4]. This process is initiated by the interaction between TCRs and

This paper is dedicated to Prof. Jürgen Brickmann, University of Technology, Darmstadt, on the occasion of his 60th birthday.

CD4 or CD8 on T cells with MHC class II or I molecules, respectively, on antigen-presenting cells (APCs) that are loaded with antigen-derived peptides [5]. However, this complex interaction itself is not sufficient for effective T cell activation, which also requires the presence of costimulatory signals delivered by CD28 and CD152 [3,4]. T cell costimulation critically depends on specific interactions between CD28 and CD152 on T cells and their ligands, CD80 and CD86, on APCs [4,6]. CD28-CD80/CD86 interactions strongly enhance TCR-dependent immune responses [3,4], whereas CD152-CD80/CD86 interactions counteract (negatively regulate) CD28-induced costimulation [7,8]. Thus, CD28/CD152-ligand interactions are critical regulatory elements of T cell activation in the course of antigen-specific immune responses [8].

CD28, CD152, and their ligands are members of the immunoglobulin (Ig) superfamily (IgSF) [9]. CD28 and CD152 molecules have a single extracellular Ig domain, whereas CD80 and CD86 have two [10]. On the cell surface, both CD28 and CD152 form covalent homodimers because of a disulphide link in the peptide segment that connects the Ig-domain to the transmembrane region. Dimerisation of CD152 and CD28 is thought to be important for the kinetics of ligand binding [6]. As predicted [11], the extracellular domain of CD152 belongs to the V(ariable)-type domain class of the IgSF [9,12]. This was confirmed by the determination of the solution structure of a monomeric form of human CD152 [13]. The three-dimensional structure of CD152 revealed the spatial arrangement of characteristic sequence motifs conserved in the CD28 family, including a non-Ig disulphide bond and the MYPPPY motif that is critical for ligand binding [13]. This structure also made it possible to construct a molecular model of CD28 [14]. On the basis of the CD152 structure and the CD28 model, residues important for binding, as identified by mutagenesis [13,15-17], were mapped and the CD80/CD86 binding site was shown to be conserved in these proteins [14].

Recently, a novel T cell surface protein, called inducible T cell costimulator or ICOS, has been identified and proposed to be a new member of the CD28 family [18]. ICOS displays 24% and 17% overall sequence identity with CD28 and CD152, respectively, and has a similar molecular organisation. Like CD28 and CD152, ICOS consists of an N-terminal signal sequence, a single extracellular domain, a linker segment, a single transmembrane domain, and a short cytoplasmic region (a total of 199 residues) [18]. Such molecular topology is quite typical for immune cell surface proteins belonging to the IgSF or other protein superfamilies [19]. More importantly, ICOS has functional characteristics similar to, yet distinct from, CD28. Expression of ICOS is T cell-restricted and, like CD28, ICOS potently amplifies T cell responses to antigen presentation by MHC molecules [18]. It costimulates T cells at levels comparable to CD28 and supports T cell-dependent proliferation of B cells, which leads to production of antibodies. However, unlike CD28, which is always expressed on the surface of most T cells, the expression of ICOS must be induced during T cell activation. Moreover, CD28 and ICOS differ in the profile of soluble cytokines whose expression they trigger. These cytokines (or lymphokines) are major mediators of T cell – T cell and T cell – B cell communication [20]. In CD28-dependent T cell activation, interleukin-2 (IL-2) predominates but ICOS mostly induces the expression of IL-10 (and not IL-2) [18]. Taken together, studies on ICOS suggest that it may play an important role at later stages of T cell activation and T cell – B cell communication [18], perhaps in conjunction with down-regulation of the CD28 signal by CD152.

Despite these functional insights, little, if anything, is currently known about the structure of ICOS and its ligand(s). It was proposed that ICOS should not bind CD80/CD86 because the MYPPPY motif was not rigorously conserved. However, this motif in CD28 and CD152 is only a part of the ligand binding site and mutating a variety of other residues abolishes binding [13, 15-17]. Thus, it was attractive to evaluate structural features of ICOS in more detail and to compare the results with CD28 and C152. Therefore, a molecular model of the extracellular Ig-like domain of ICOS was constructed and analysed. Several questions were of interest and investigated with the aid the model. For example, given the low sequence identity shared by ICOS and CD28/CD152, how similar are their structures? Are functionally important residues conserved and, if so, where do they map? How does the binding site in CD28/CD152 compare with corresponding regions in ICOS? How are glycosylation sites distributed in the extended CD28 family? Thus, focal points of the study presented herein were the three-dimensional analysis and comparison of conserved residues and functionally important regions.

Methods

Sequences of CD28 and CD152 from different species were obtained from GeneBank [21] and Swiss-Prot [22] and compared with ICOS (PIR accession number S78540). Sequences of the Ig-like domains were aligned using the sequence-structure alignment function of MOE [23]. The alignment was manually modified to match IgSF consensus positions [9] and other core residues important for structural integrity of CD152 [13]. A figure containing the sequence alignment was produced with Microsoft Excel. Coordinates of an ensemble of NMR structures of CD152 were obtained from the Brookhaven Protein Data Bank [24] (PDB entry 1AH1). As discussed below, the local structure of only one segment in CD152 was not well defined in the NMR-derived models. As template for model building of ICOS, an averaged energy minimised NMR structure of CD152 was used that displayed good stereochemistry and no short intramolecular contacts. An averaged NMR structure of CD152 was also used previously to build a molecular model of CD28 [14].

Computer graphics and model building were carried out with WebLab Viewer Lite [25] and MOE. Backbone segments conserved in CD28, CD152 and ICOS were identified on the basis of consensus residue matches and selected from the averaged NMR structure of CD152. These regions pro-

vided the core of the ICOS model. Side chain replacements were carried out in standard rotamer conformations [26]. Non-conserved regions in ICOS include the A'-B, B-C, and D-E loops, the deletion of the C-C' loop, and a one residue deletion at the beginning of the G-strand (see Results). Approximate conformations of these regions were modelled using suitable fragments (i.e., same length, similar sequence, good stereochemistry, close spatial fit to the framework termini) extracted from PDB structures. These database searches were performed using the homology modelling function of MOE that combines a segment matching technique [27] with α-carbon distance matrix comparisons [28]. The assembled ICOS model was energy minimised using the MOE force field [29] with complete hydrogen atom representation until the root mean square (rms) derivative of the energy function was approximately 1 kcal mol^{-1} $Å^{-1}$. Following energy minimisation, hydrogen atoms were removed. Stereochemistry and intramolecular contacts were analysed using PROCHECK

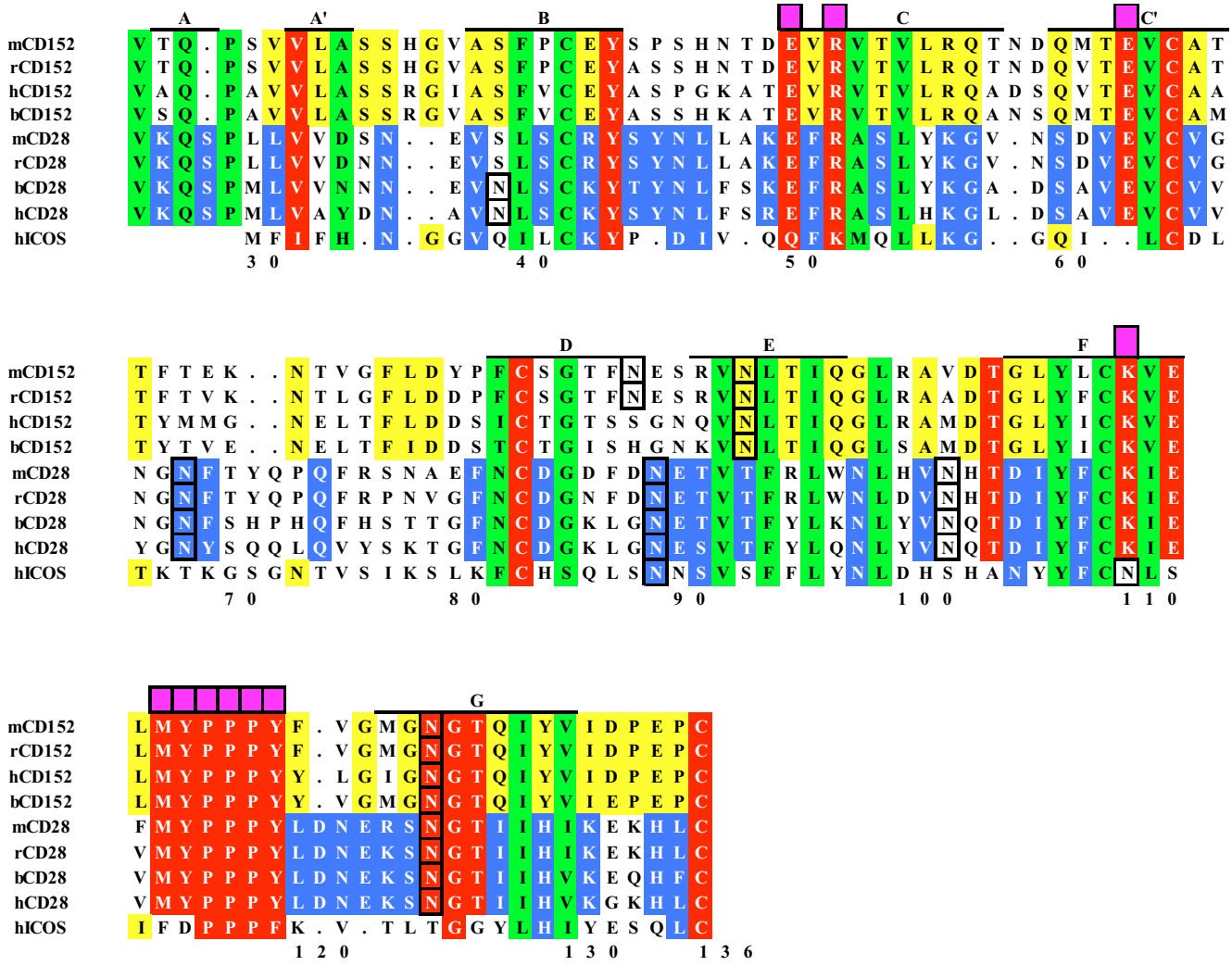

Figure 1 *Sequence comparison of the extended CD28 family. Sequences of the Ig-like domains of human ICOS (hICOS) and CD28 and CD152 molecules from different species (m, mouse; r, rat; h, human; b, bovine) were aligned taking the NMR structure of CD152 [13] into account. The β-strands in CD152 are shown and labelled according to IgSF nomenclature [9]. Residue numbers are given for ICOS. IgSF V-set consensus residue positions and additional hydrophobic core residues are highlighted in green. Conserved residues outside IgSF signature positions are shown in red. Residues only conserved in CD28 (and ICOS) are shown in blue and residues only conserved in CD152 (and ICOS) in yellow. The most conserved residue replacements (e.g., Y/F or R/K) were taken into account. Magenta boxes indicate conserved residues that are particularly important for CD80/CD86 binding to CD28 and CD152, as identified by mutagenesis. Potential N-linked glycosylation sites are boxed.*

[30] and structural superpositions were calculated with ALIGN [31].

In order to study the spatial arrangement of N-linked glycans in the CD28 family, a glycan core structure was attached to N-linked glycosylation sites in the CD28 and ICOS models using MOE. As glycan core, an NMR-derived model of a tetrasaccharide [mannose-(β1-4)-N-acetyl-glucosamine-((β1-4)-N-acetyl-glucosamine)-(α1-6)-fucose] was selected. This structure was bound to CD152 and resulted from partial deglycosylation of N-glycans [13]. Protein-carbohydrate contacts were, if necessary, improved by minor energy minimisation with protein atoms held fixed.

Results and discussion

Structural features of CD152 and CD28

The extracellular domain of CD152 adopts an Ig V-like fold [13], which consists of two β–sheets with four (A-B-E-D) and six (A'-G-F-C-C'-C") β–stands, respectively. This folding type is determined by characteristic Ig V-set consensus residues [9] and those residues distinguish it from other Ig structure classes [12]. In addition, CD152 has some unique features. It includes a non-canonical disulphide bond that tethers the C'-strand to the D-strand. Furthermore, the region encompassing the C'-C" loop and C"-strand at the edge of the β-sheet is highly flexible in the solution structure and the C"-strand (which lacks interactions with the hydrophobic core) is not formed [13]. The Ig-domains of human CD152 and CD28 share approximately 27% sequence identity and most of the IgSF consensus and other core residues, leaving little doubt that their structures are very similar [14].

Sequence comparison

A structure-based sequence alignment of Ig domains of CD28 and CD152 from different species and human ICOS is shown in Figure 1. The figure highlights IgSF consensus residues and conservation of residues outside consensus positions. In the aligned region, ICOS and CD28 (CD152) display approximately 24% (17%) sequence identity. Most Ig V-set consensus residues are conserved, or conservatively replaced, in ICOS, consistent with the idea that the extracellular domain of ICOS also adopts a V-fold. CD152 is likely to be a good structural template for ICOS because the non-canonical disulphide bond (C63-C83; in addition to the canonical Ig disulphide bond C42-C109) and the structurally important leucine residue in the E-F loop are conserved. The presence of these structural elements in CD152 causes some departures from typical Ig V-fold geometry [13]. These features together with the conservation of IgSF V-set consensus residues suggest that the structures of CD152 and ICOS are similar, despite relatively low sequence identity. When only conservation outside IgSF signature residues is considered (which determine structure but not binding specificity), the sequence identity between ICOS and CD28 (CD152) is only approximately 17% (10%). At this low level of sequence identity, it is often difficult to decide whether sequence similarities are functionally relevant or occurrence by chance [32], thus making a more detailed analysis necessary. However, although sequence identity is low in this case, the alignment of ICOS relative to CD152 and CD28 is unambiguous, due to the conservation of IgSF consensus residues and signature residues of the CD28 family. If it is possible to generate topologically correct sequence alignments [19,33], reasonable molecular models can be generated even if sequence identities shared by template and target structures are only 20-30% [34-36].

Model building

The modelled region of ICOS includes residues 30-132. The model displays good stereochemistry and intramolecular contacts. Using ALIGN, 94 residues can be superposed on corresponding positions in CD152 with an α-carbon rms deviation of 0.8 Å. Figure 2 shows a superposition of the CD152 structure and CD28 and ICOS molecular models. The average backbone conformation of the C'-C" region, which is highly flexible in CD152, was retained in the model. For the

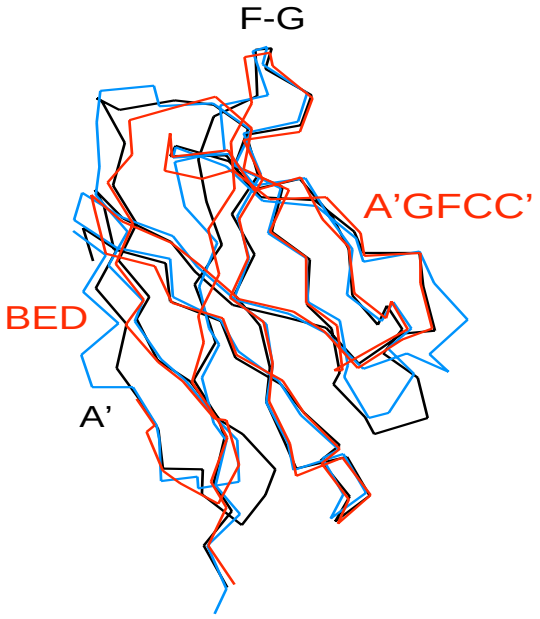

Figure 2 *Comparison of ICOS, CD152, and CD28. Alpha–carbon traces of the structure of CD152 (black) and molecular models of CD28 (blue) and ICOS (red) are shown after optimal superposition. The view is from the side approximately along the interface of the two β–sheets of the domains. The BED and A'GFCC' β–sheet surfaces in ICOS are labelled as well as the positions of the A'-strand and F-G loop (see also "Supplementary material available").*

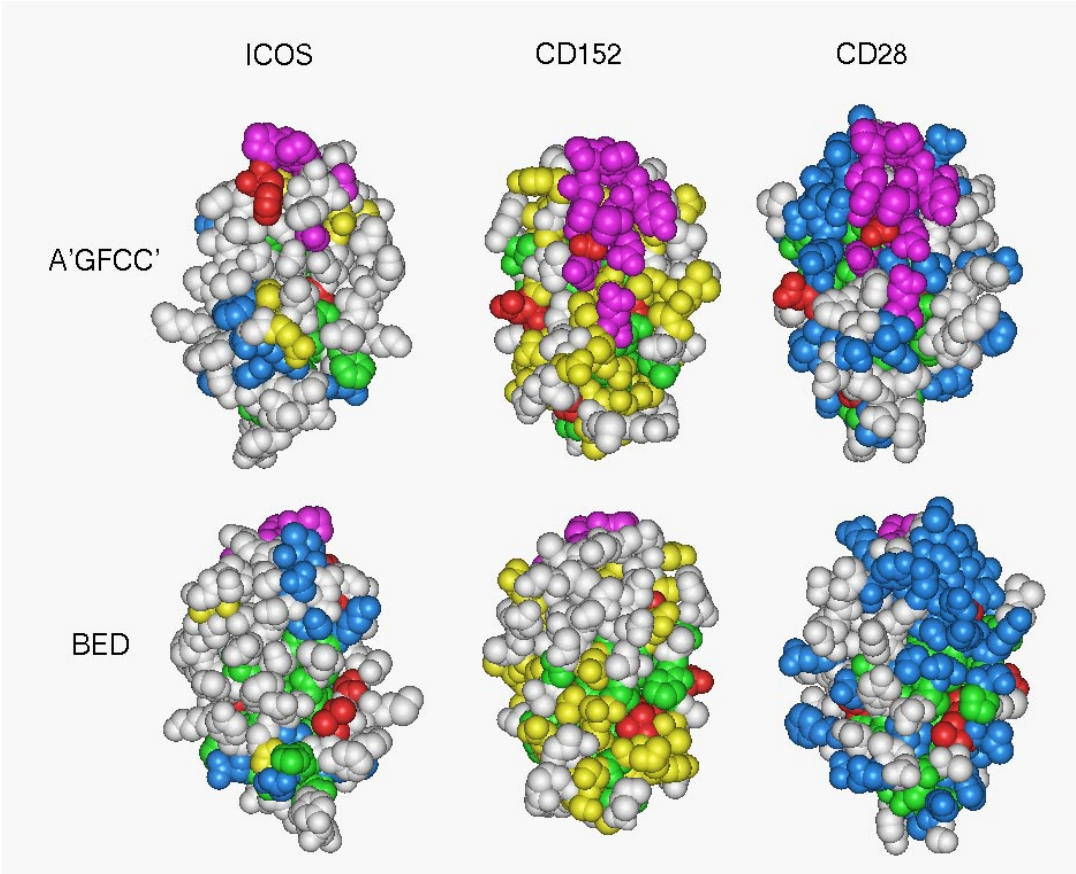

Figure 3 *Conservation of residues in the CD28 family. ICOS, CD152, and CD28 are shown in equivalent orientation and space-filling representation. IgSF consensus positions and conserved residues are mapped on the structures following the classification and colour code of Figure 1. IgSF consensus and core residues are shown in green, residues conserved in CD152, CD28, and ICOS in red, residues conserved only in CD152 (and ICOS) in yellow, and residues conserved only in CD28 (and ICOS) in blue. Residues conserved in CD152 and CD28 important for CD80/CD86 binding are coloured magenta. Both β–sheet surfaces are viewed (top: A'GFCC' face; bottom: BED face of ICOS, corresponding to the ABED face of CD152 and CD28). The top and bottom views are related by approximately 180° rotation around the vertical axis.*

B-C loop that is not conserved in ICOS and CD152, only constrained backbone conformations could be identified by database searching, given the end point geometry of the loop, its length, and composition. The modelled conformation was considered tentative and residues 46-48 were omitted from the final model. By contrast, several similar database segments were available to model the one residue deletion in ICOS in the C-terminal segment of the F-G loop following the conserved triple proline motif. In the model, the trans-trans-cis conformation of the PPP motif in CD152 was retained. ICOS lacks the proline residue that marks the transition of the A- to the A'-strand and the strand switch from one β–sheet to the other that is usually seen in Ig V-domains [12]. Furthermore, A-strand IgSF consensus residues are not found in ICOS, indicating that the A-strand is not formed. Similar observations have been made for other cell surface proteins belonging to the IgSF, for example, CD2 and CD58, which also lack an A-strand [37]. No A-strand was modelled and residue M30 marks the beginning of the A'-strand in ICOS. Thus, the modelled Ig domain of ICOS is composed of two β-sheets, the A'GFCC' sheet and the BED sheet that are connected by loops following conserved Ig V-type topology [9]. Residue C134 (six positions C-terminal of the G-strand) is conserved in ICOS, CD152, and CD28 and responsible for the formation of the disulphide bond that dimerises their domains on the cell surface [13].

Conservation of protein surface residues

Using the ICOS model, conservation of residues in the extended CD28 family was studied. Figure 3 shows a side-by-side comparison of ICOS, CD152, and CD28. Only residues on the protein surface outside IgSF consensus positions can determine the binding specificity of these receptors. The A'GFCC' β–sheet surface in CD152 and CD28 is extended

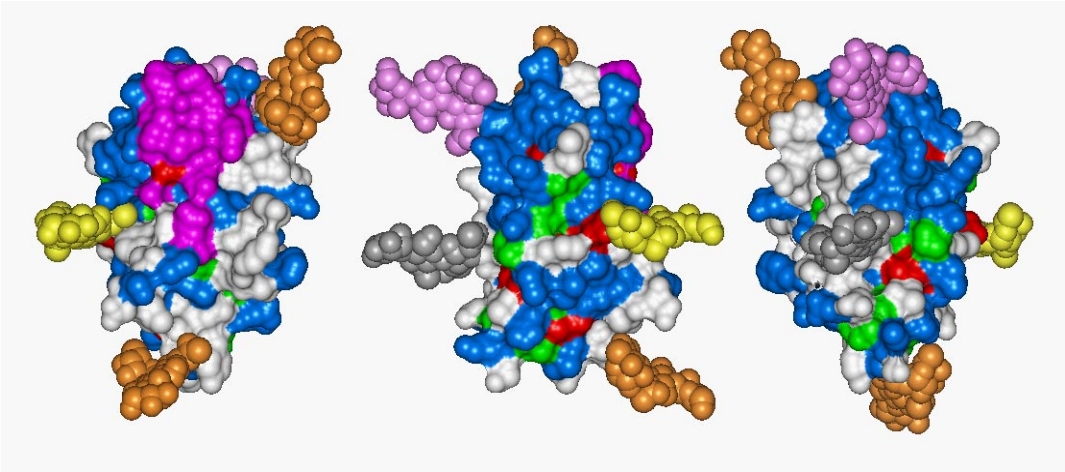

Figure 4 *Spatial arrangement of N-linked glycosylation sites in CD28. The model is shown with solvent-accessible surface (probe radius 1.4 Å) [39] and the same colour code as in Figure 3. Five N-linked glycans in human CD28 are approximated as tetrasaccharide core structures and shown in space-filling representation. Glycans are colour-coded (yellow, gold, silver, pink) with respect to their conservation in CD152 and ICOS. The yellow glycan is conserved in CD152 and the pink glycan is conserved in ICOS. The position of the silver glycan approximately corresponds to the position of the second glycan in CD152. Gold glycans are unique to CD28. The left view focuses on the A'GFCC' β–sheet surface that contains the CD80/CD86 binding site. From the left to the right, the CD28 model is rotated in 90° increments so that the view on the right shows the ABED face of the domain.*

by the F-G loop that contains the MYPPPY motif. The upper part of this face is highly conserved in CD152 and CD28 and forms the center of the binding site for CD80 and CD86 [13]. The A'GFCC' face has been shown to contain binding sites in a variety of cell surface receptors and adhesion molecules belonging to the IgSF, regardless of the structure of their ligands [38]. In ICOS, the critical MYPPPY motif is partly conserved (i.e., FDPPPF) but the majority of other CD152/CD28 residues that form the CD80/CD86 binding site are not conserved. This suggests that ICOS does not bind these ligands. CD152 and CD28 molecules also have largely conserved surface patches outside the CD80/CD86 binding site. The upper parts of the A'GFCC' face and the opposite BED face display strong conservation in CD28, while the A'GFCC' face and the lower part of the BED face are mostly conserved in CD152. Overall, residue conservation is greater on the A'GFCC' than the BED face. ICOS shows spurious conservation of CD28 and/or CD152 surface residue positions throughout the domain but no strongly conserved region. It appears that all surface patches conserved in CD28 and CD152 or only in CD28 have some residual residue conservation in ICOS. Conservation is least obvious in regions that are conserved in CD152 only, most notably the lower part of the BED surface. This supports the idea that ICOS is more closely related to CD28 than to CD152.

Distribution of N-linked glycosylation sites

Glycosylation of CD152 is important to prevent its aggregation in solution but does not directly participate in CD80/CD86 binding [13]. CD152 has two N-linked glycosylation sites, one in the G-strand (conserved in CD28) and one in the E-strand that is exposed on the BED face [13]. By contrast, human CD28 has five N-linked glycosylation sites. In order to study their spatial arrangement relative to conserved residues, glycan core structures were modelled, as shown in Figure 4. Branched N-linked carbohydrates are much larger than the tetrasaccharide core structures shown here. Nevertheless, these structures provide a view of the spatial constraints imposed by N-linked glycosylation and illustrate how glycans limit the accessibility of the protein surface. Figure 4 shows that the CD80/CD86 binding site in CD28 is, as to be expected, not covered by N-linked glycans. Glycosylation sites are peripheral to this region but do not mask the binding site. By contrast, an N-linked glycan, the position of which approximately corresponds to one in CD152, maps to the center of the BED face and limits access to this region. In addition, another glycan in CD28 that is conserved in ICOS maps to the top of the BED face. Like CD152, ICOS has only two N-linked glycosylation sites, and modelled glycans are shown in Figure 5. In addition to the glycosylation site at N89 on the BED face that is conserved in CD28, a second site at N110 is located on the opposite A'GFCC' face. N110 in ICOS replaces a lysine that is conserved in CD28 and CD152 and critical for CD80/CD86 binding (Figure 1). The N-linked glycan bound to N110 in ICOS maps to the center of the region that corresponds to the ligand binding site in CD28 and CD152 and masks this site (Figure 5). Thus, this region is not be available for ligand binding to ICOS, although it can not be ruled out that N-linked carbohydrates participate in ICOS-ligand interactions. As shown in Figures 3 and 5,

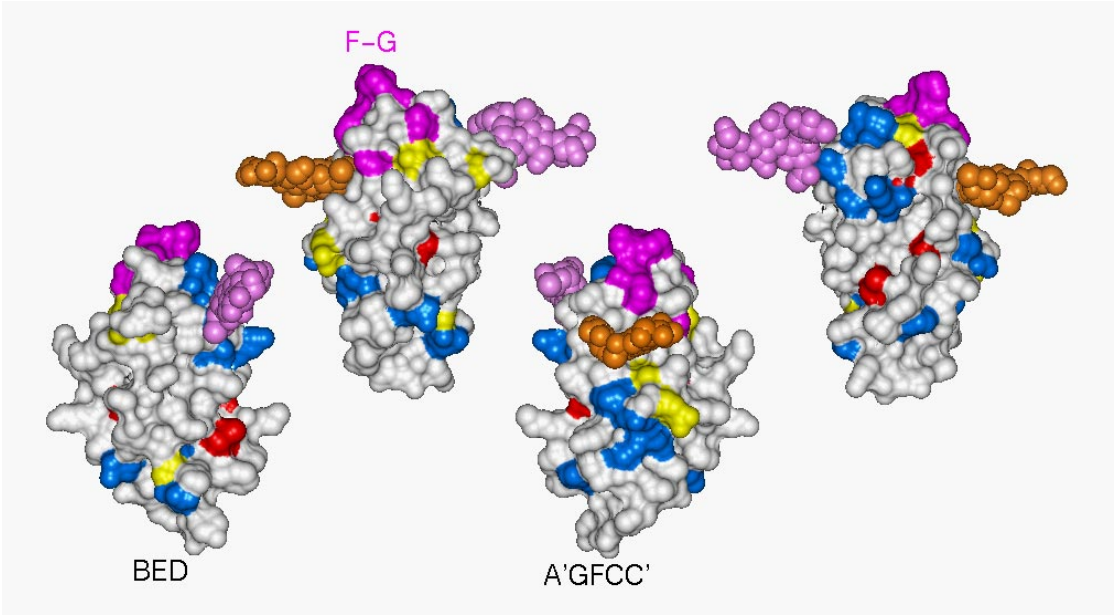

Figure 5 *Glycosylation sites and conserved residues in ICOS. The model is shown with solvent-accessible surface (probe radius 1.4 Å) [39] and colour-coded, as in Figure 3, except that IgSF consensus residues (green in Figure 3) are not highlighted here. The view on the left focuses on the BED face. From the left to the right, the model is rotated in 90° increments around the vertical axis (i.e., BED face is followed by a side view, the A'GFCC' face, and another side view). In this orientation, the F-G loop including the conserved triple proline motif (magenta) is at the top and the C-terminus (i.e., membrane-proximal region) of the domain at the bottom. N-linked glycan core structures (shown in space-filling representation) map to the upper part of the BED face (pink, conserved in CD28; see also Figure 4) and the A'GFCC' face (gold, unique to ICOS).*

the lower part of the BED face in ICOS contains very few conserved residues and no glycosylation site. Thus, it is the most unique surface area in ICOS.

Dimerisation

As mentioned above, CD28, CD152, and ICOS form disulphide-linked dimers on the cell surface. An engineered form of CD152 lacking this disulphide link is predominantly monomeric in solution [13], suggesting that non-covalent dimerisation is weak, if at all present. It is currently unknown whether a conserved dimer interface exists in the CD28 family or at least a preferred relative orientation of the domains on the cell surface. The residue mapping studies reported here do not predict a preferred domain orientation, if it exists, but help to rule out some possibilities. The distribution of glycosylation sites and residues important for binding suggests that neither β–sheet surface is available to preferentially orient the domains or support covalent dimerisation. The A'GFCC' face contains the ligand binding site in CD28 and CD152 and should thus not be involved in dimerisation. Moreover, in ICOS, the corresponding region is masked by an N-linked glycan. The opposite BED faces of these domains also carry either one or two N-linked glycans. Thus, a face-to-face interaction of the Ig domains is not likely. In CD28 and CD152, the conserved glycosylation site in the G-strand would also prevent dimer formation involving this region. However, a lateral (i.e., side-by-side) arrangement of domains, for example, along the site opposite to the G-strand may be possible. On the other hand, an important function of N-linked glycans could be to sufficiently space the covalently linked domains so that simultaneous binding or rebinding of ligands is readily possible, consistent with fast kinetic on- and off-rates of binding observed for these receptors [6].

Evolutionary implications

Taken together, the findings discussed above make it possible to draw some conclusions regarding the evolution of the extended CD28 family. Conservation of IgSF consensus residues and other features suggests that the structures of extracellular regions of members of the CD28 family are quite similar. However, the distribution of conserved and non-conserved surface residues is consistent with the idea that ICOS has diverged from CD28 during evolution earlier than CD152, which has preserved the CD80/CD86 binding specificity. However, CD152 has developed a different signalling function, due to changes in its cytoplasmic region, and negatively regulates CD28-mediated T cell costimulation. By contrast, ICOS has substantially diverged from CD28 and very likely

recognises ligand(s) other than CD80/CD86 by a different mechanism. Nevertheless, ICOS enhances T cell functions in a way similar to, yet distinct from, CD28. This illustrates the rather complex manner in which the CD28 family enhances and regulates T cell functions and T cell – B cell communication.

Acknowledgement I thank Peter Linsley, Rosetta Inpharmatics, for longstanding collaborations on understanding the structure and binding characteristics of the CD28 family.

Supplementary material available Coordinates of the molecular model of ICOS have been deposited with the *Journal*. The model is also available from the author via e-mail upon request. In addition, a stereo version of Figure 2 of the manuscript is available as a postscript file from the author.

References

1. Aruffo, A.; Seed, B. *Proc. Natl. Acad. Sci. USA* **1987**, *84*, 8573.
2. Brunet, J. F.; Denizot, F.; Luciani, M. F.; Roux-Dosseto, M.; Suzan, M., Mattei, M. G.; Goldstein, P. *Nature* **1987**, *328*, 267.
3. Linsley, P. S.; Ledbetter, J. A. *Ann. Rev. Immunol.* **1993**, *11*, 191.
4. Lenschow, D. J.; Walunas, T. L.; Bluestone, J. *A. Ann. Rev. Immunol.* **1996**, *14*, 233.
5. Marrack, P.; Kappler, J. *Adv. Immunol.* **1986**, *38*, 1.
6. Linsley, P. S.; Ledbetter, J.; Peach, R.; Bajorath, J. *Res. Immunol.* **1995**, *146*, 130.
7. Walunas, T. L.; Lenschow, D. J.; Bakker, C. Y.; Linsley, P. S.; Freeman, G. J.; Green, J. M.; Thompson, C. B.; Bluestone, J. A. *Immunity* **1994**, *1*, 405.
8. Thompson, C. B.; Allison, J. P. *Immunity* **1997**, *7*, 445.
9. Williams, A. F.; Barclay, A. N. *Ann. Rev. Immunol*. **1988**, *6*, 381.
10. Bajorath, J.; Peach, R. J.; Linsley, P. S. *Protein Sci.* **1994**, *3*, 2148.
11. Bajorath, J.; Linsley, P. S. *J. Mol. Model.* **1997**, *3*, 117.
12. Bork, P.; Holm, L.; Sander, C. *J. Mol. Biol.* **1994**, *242*, 309.
13. Metzler, W. J.; Bajorath, J.; Fenderson, W.; Shaw, S.-Y.; Constantine, K. L.; Naemura, J.; Leytze, G.; Peach, R. J.; Lavoie, T. B.; Mueller, L.; Linsley, P. S. *Nature Struct. Biol.* **1997**, *4*, 527.
14. Bajorath, J.; Metzler, W. J.; Linsley, P. S. *J. Mol. Graph. Model.* **1997**, *15*, 135.
15. Peach, R. J.; Bajorath, J.; Brady, W.; Leytze, G.; Greene, J.; Naemura, J.; Linsley, P. S. *J. Exp. Med.* **1994**, *180*, 2049.
16. Morton, P. A.; Fu, X.-T.; Stewart, J. A;, Giacoletto, K. S.; White, S. L.; Leysath, C. E.; Evans, R. J.; Shieh, J.-J.; Karr, R. W. *J. Immunol.* **1996**, *156*, 1047.
17. Kariv, K.; Truneh, A.; Sweet, R. W. *J. Immunol.* **1996**, *157*, 29.
18. Hutloff, A.; Dittrich, A. M.; Beier, K. C.; Eljaschewitsch, B.; Kraft, R.; Anagnostopoulos, I.; Kroczek, R. A. *Nature* **1999**, *397*, 263.
19. Bajorath, J. *J. Mol. Model.* **1998**, *4*, 1.
20. Thompson, C. B.; Lindsten, T.; Ledbetter, J. A.; Kunkel, S. L.; Young, H. A.; Emerson, S. G.; Leiden, J. M.; June, C. H. *Proc. Natl. Acad. Sci. USA* **1989**, *86*, 1333.
21. Benson, D. A.; Boguski, M. S.; Lipman, D. J.; Ostell, J.; Ouellette, B. F. *Nucl. Acid Res.* **1998**, *26*, 1.
22. Bairoch, A.; Apwiler, R. *Nucl. Acid Res.* **1999**, *27*, 49.
23. MOE, Molecular Operating Environment, Version 1999.05, Chemical Computing Group, Inc., 1255 University Street, Suite 1600, Montreal, Quebec, Canada, H3B, 3X3 (http://www.chemcomp.com).
24. Bernstein, F. C.; Koetzle, T. F.; Williams, G. J. B.; Meyer, E. F., Jr.; Brice, M. D.; Rodgers, J. R.; Kennard, O.; Shimanouchi, T.; Tasumi, M. *J. Mol. Biol.* **1977**, *112*, 535.
25. WebLab Viewer Lite, 1999, MSI, 9685 Scranton Road, San Diego, California, USA (available from: http://www.msi.com/solutions/products/weblab/viewer).
26. Ponder, J. W.; Richards, F. M. *J. Mol. Biol.* **1987**, *193*, 775.
27. Levitt, M. *J. Mol. Biol.* **1992**, *226*, 507.
28. Jones, T. A.; Thirup, S. *EMBO J.* **1986**, *5*, 819.
29. Labute, P. MOE Forcefield Facilities (http://www.chemcomp.com/article/ff.htm). Chemical Computing Group, Chemical Computing Group, Inc., 1255 University Street, Suite 1600, Montreal, Quebec, Canada, H3B, 3X3.
30. Laskowski, R. A.; MacArthur, M. W.; Moss, D. S.; Thornton, J. M. *J. Appl. Cryst.* **1993**, *26*, 283.
31. Satow, Y.; Cohen, G. H.; Padlan, E. A. *J. Mol. Biol.* **1986**, *190*, 593.
32. Doolittle, R. F. *Science* **1981**, *214*, 149.
33. Bajorath, J.; Stenkamp, R.; Aruffo, A. *Protein Sci.* **1993**, *2*, 1798.
34. Bajorath, J.; Stenkamp, R.; Aruffo, A. *Bioconjug. Chem.* **1995**, *6*, 3.
35. Bajorath, J.; Linsley, P. S.; Metzler, W. J. *J. Mol. Model.* **1997**, *3*, 287.
36. Bajorath, J. *J. Biol. Chem.* **1998**, *273*, 24603.
37. Wang, J.; Smoylar, A.; Tan, K.; Liu, J.; Kim, M.; Sun, Z. J.; Wagner, G.; Reinherz, E. L. *Cell* **1999**, *97*, 791.
38. Skonier, J. E.; Bowen, M. A.; Emswiler, J.; Aruffo, A.; Bajorath, J. *Biochemistry* **1996**, *35*, 12287.
39. Connolly, M. *Science* **1983**, *221*, 709.